Interconnected Ionic Domains Enhance Conductivity in Microphase Separated Block Copolymer Electrolytes

Christopher G. Arges[a], *Yu Kambe*[b,c], *Moshe Dolejsi*[b,c], *Guangpeng Wu*[d], *Tamar Segal-Pertz*[b,c], *Jiaxing Ren*[b,c], *Chi Cao*[a], *Gordon S.W. Craig*[b], *and Paul F. Nealey*[b,c]

[a]Cain Department of Chemical Engineering, Louisiana State University, Baton Rouge, LA 70803

[b]Institute for Molecular Engineering, University of Chicago, Chicago, IL 60637

[c]Materials Science Division, Argonne National Laboratory, Argonne, IL 60439

[d]Department of Polymer Science and Engineering, Zhejiang University, Hangzhou, China, 310027

Electronic Supporting Information

Supplemental Data

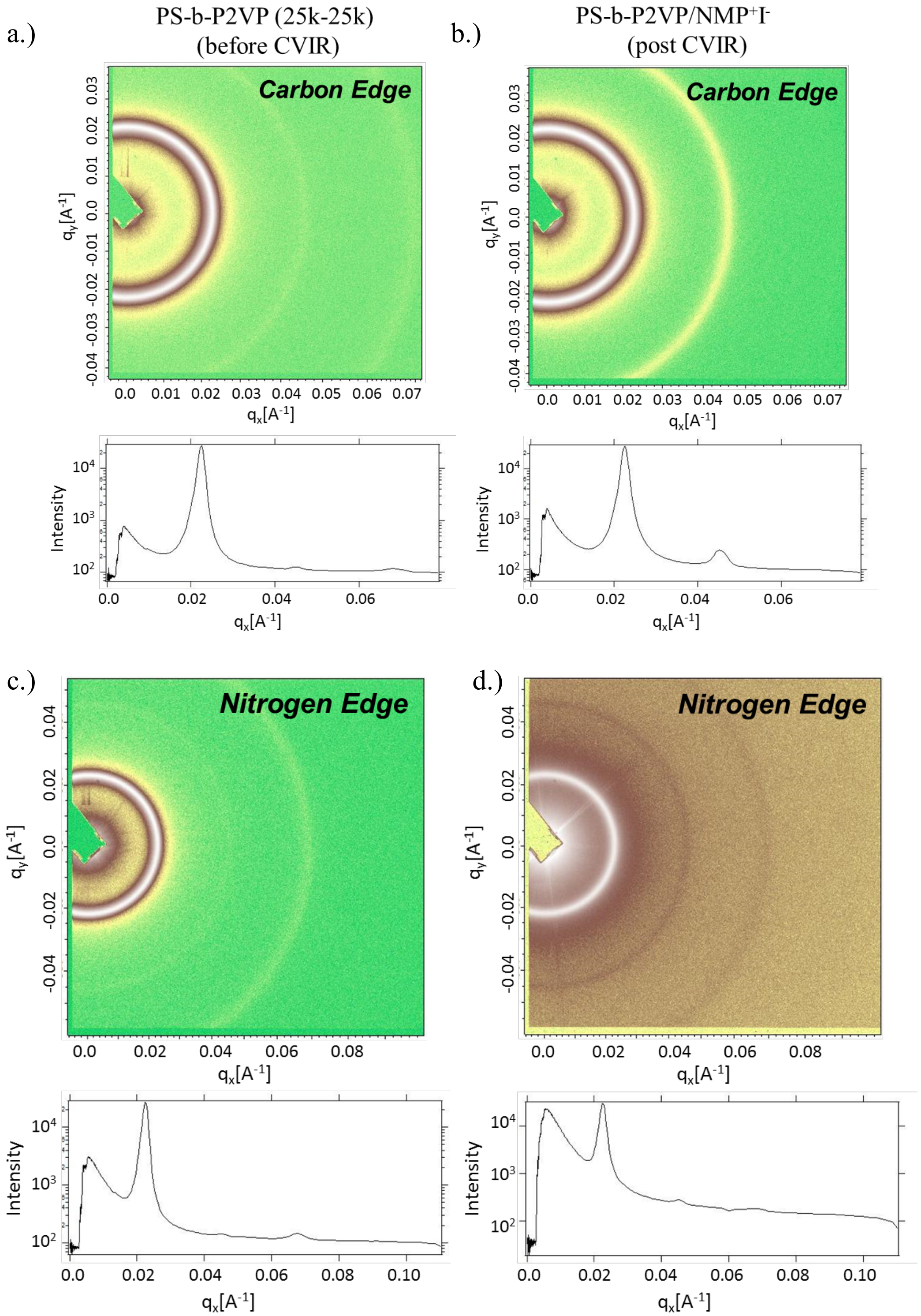

Figure S1. RSoXS patterns near the carbon edge for a.) PS-*b*-P2VP (diblock 25-*b*-25 kg/mol, before CVIR) and b.) PS-*b*-P2VP/NMP$^+$ I$^-$ (after the CVIR reaction). Panels c.) and d.) are the respective RSoXS patterns near the nitrogen edge.

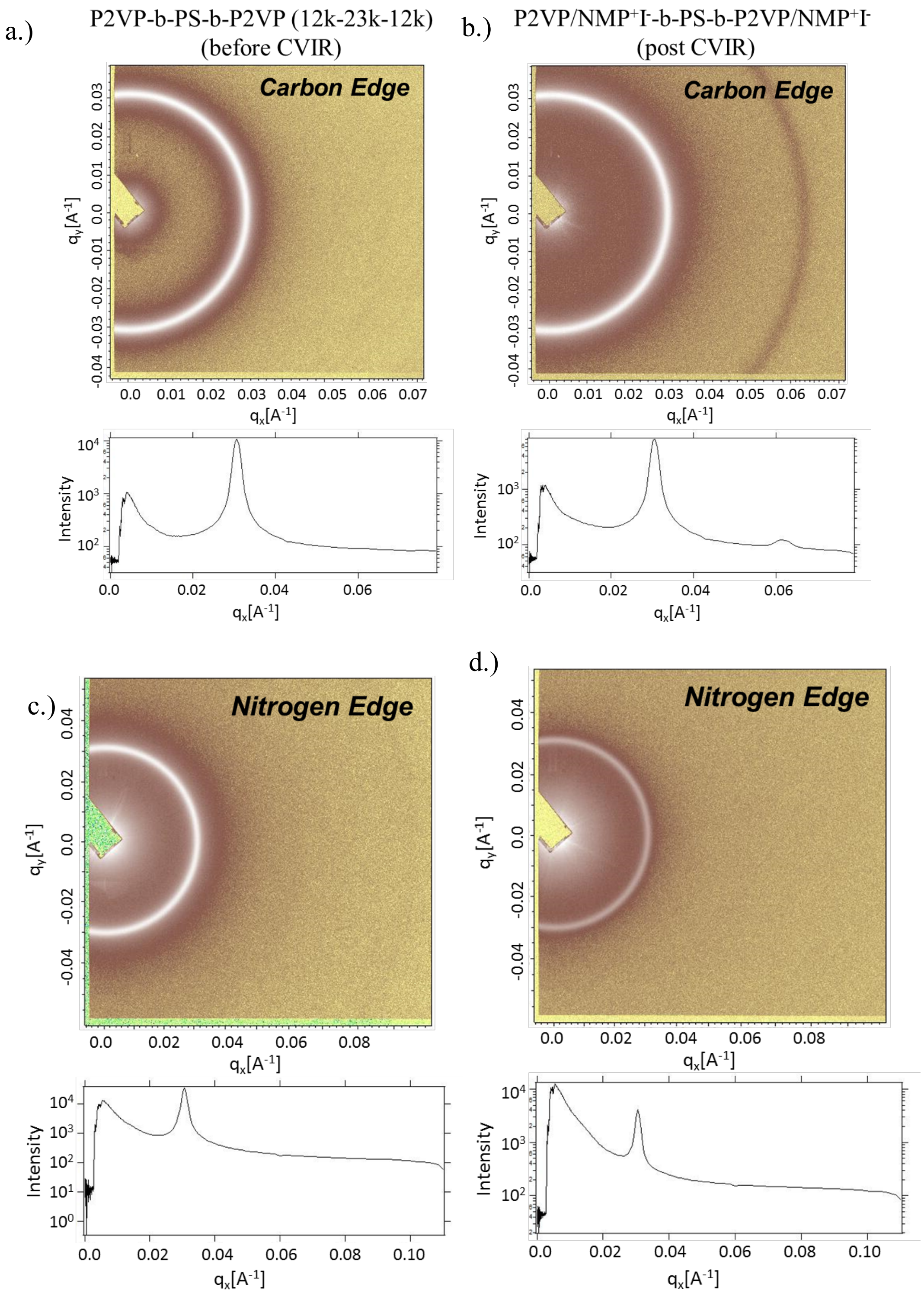

Figure S2. RSoXS patterns near the carbon edge for a.) P2VP-*b*-PS-*b*-P2VP (M_n = 12-*b*-23-*b*-12 kg/mol – before CVIR) and b.) P2VP/NMP$^+$ I$^-$-*b*-PS-*b*-P2VP/NMP$^+$ I$^-$ (after the CVIR reaction). Panels c.) and d.) are the respective RSoXS patterns near the nitrogen edge.

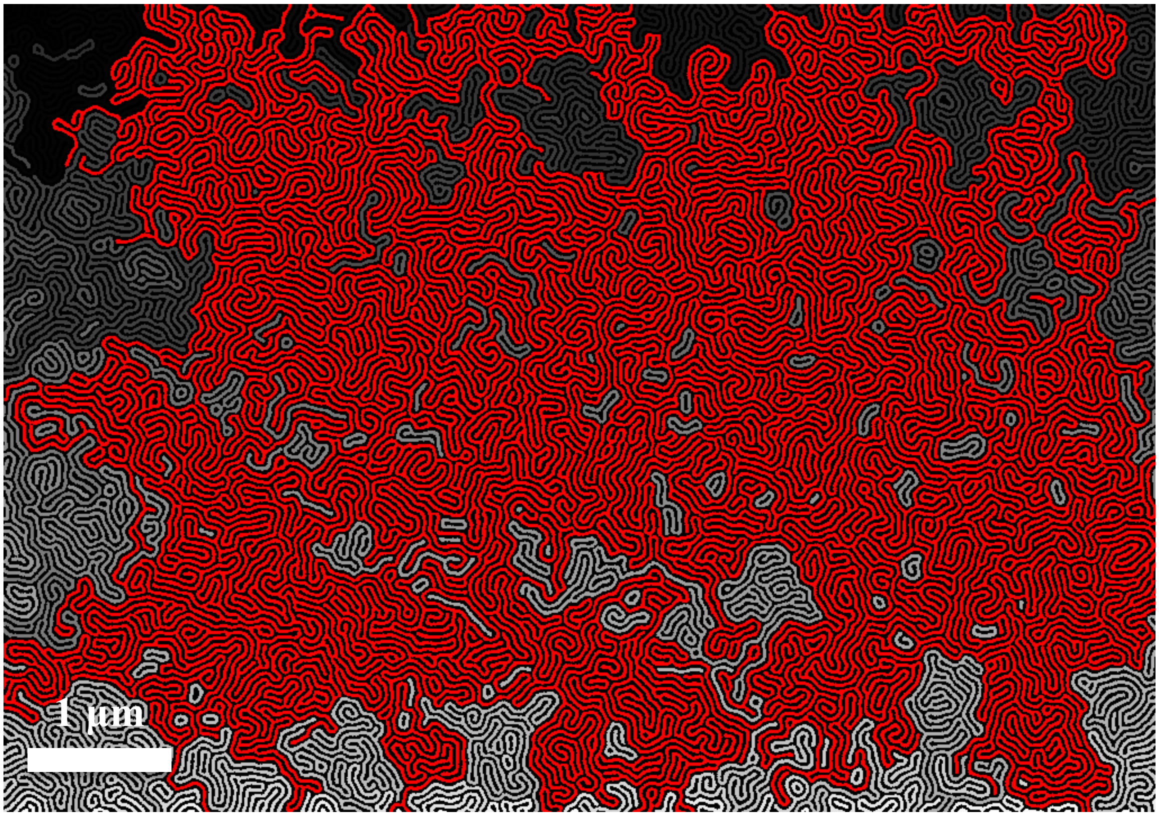

Figure S3. Processed SEM image (taken from collected 8 μm x 8 μm images) of self-assembled PS-*b*-P2VP/NMP^{+} I^{-} with a targeted P2VP volume fraction of 45%.

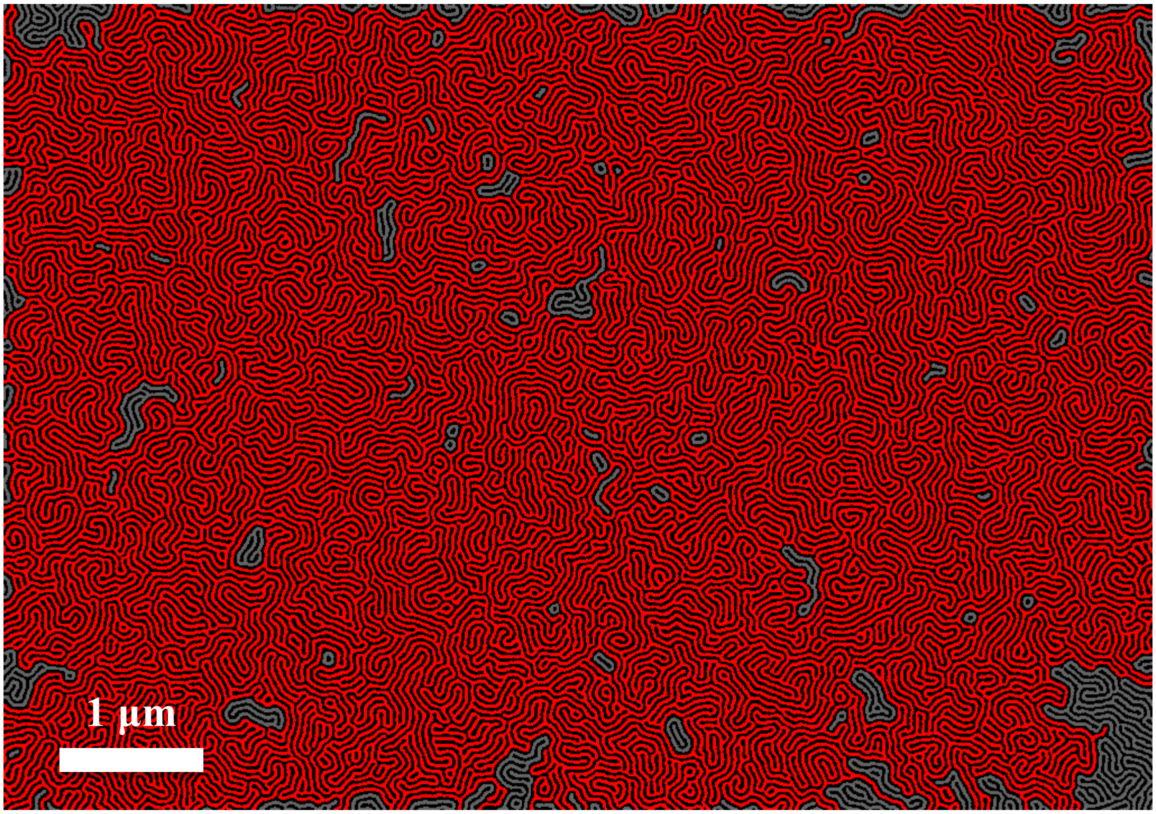

Figure S4. Processed SEM image (taken from collected 8 μm x 8 μm images) of self-assembled PS-*b*-P2VP/NMP$^+$ I$^-$ with a targeted P2VP volume fraction of 47.5%.

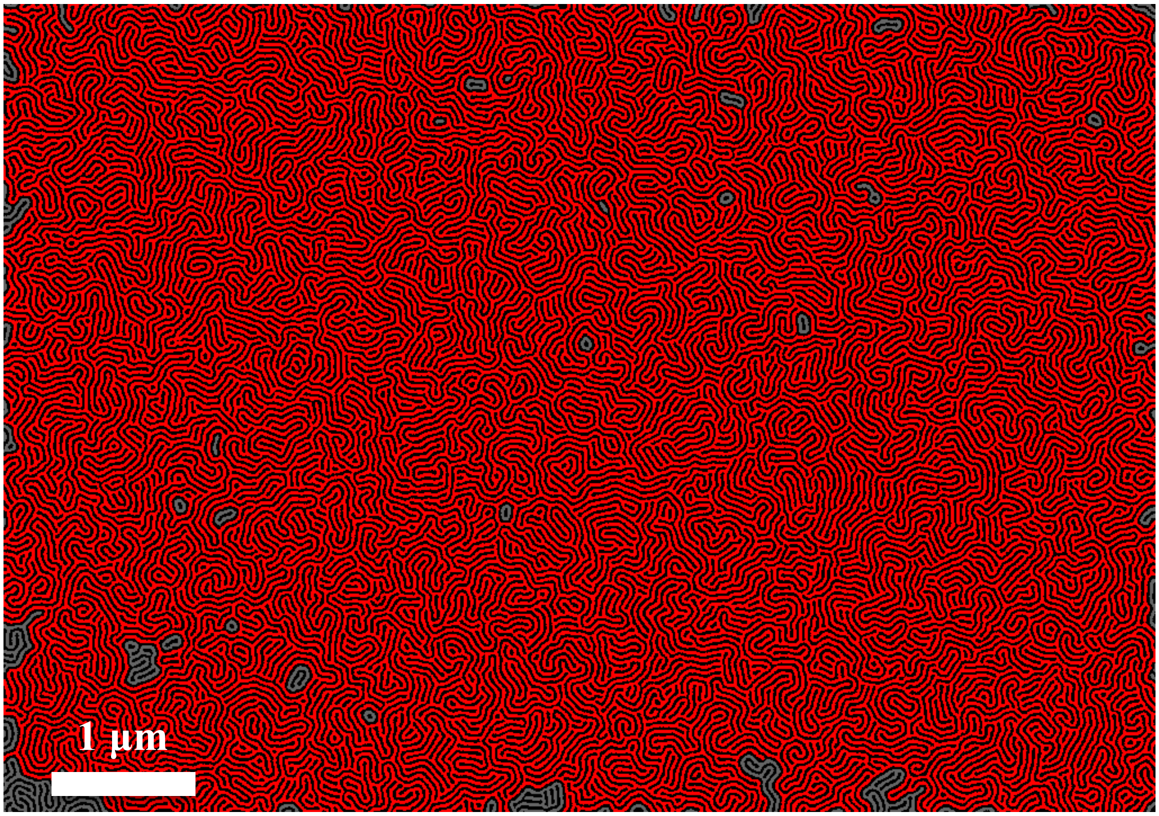

Figure S5. Processed SEM image (taken from collected 8 µm x 8 µm images) of self-assembled PS-*b*-P2VP/NMP$^+$ I$^-$ with a targeted P2VP volume fraction of 50%.

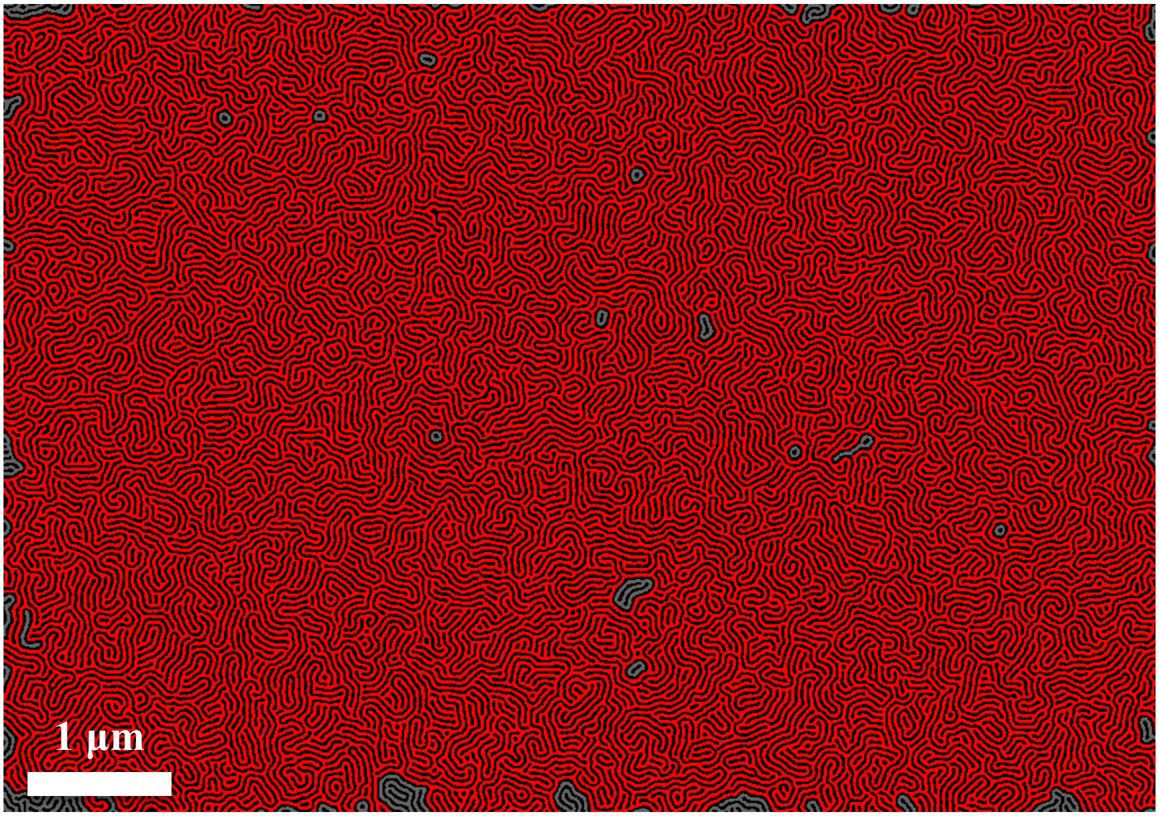

Figure S6. Processed SEM image (taken from collected 8 µm x 8 µm images) of self-assembled PS-*b*-P2VP/NMP$^+$ I$^-$ with a targeted P2VP volume fraction of 52.5%.

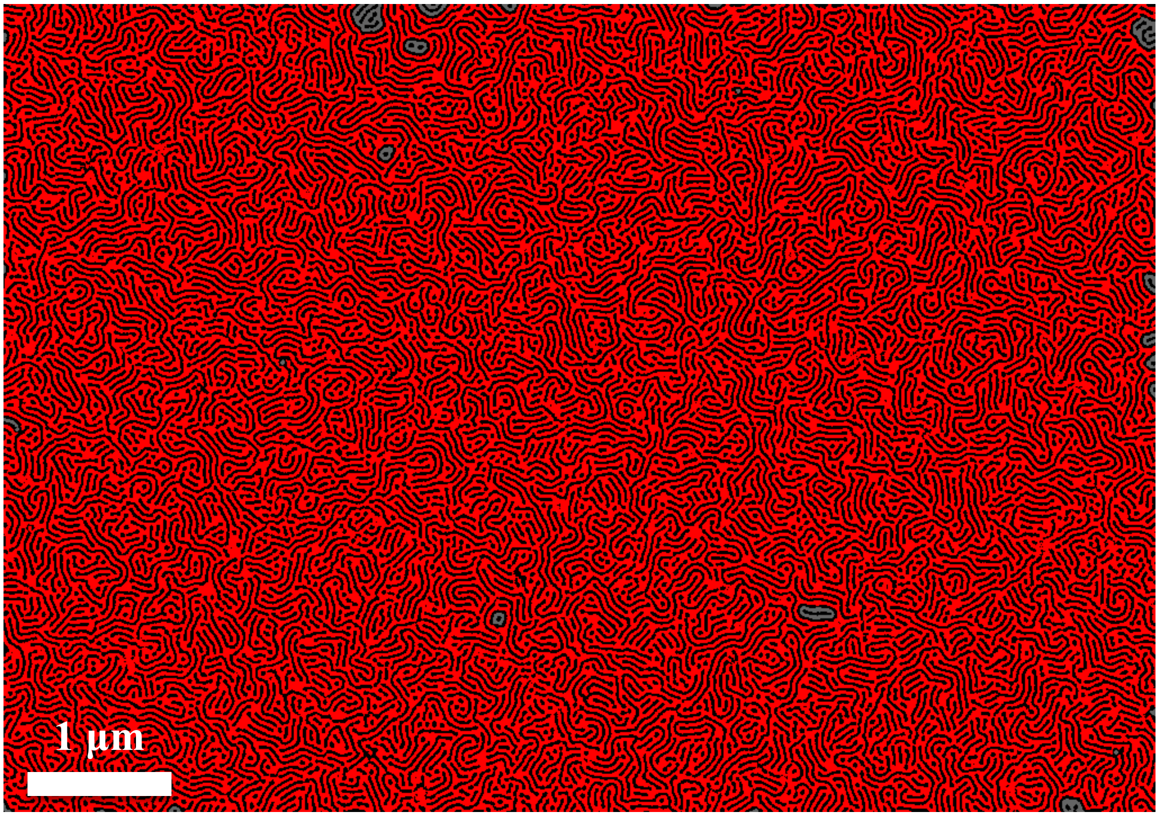

Figure S7. Processed SEM image (taken from collected 8 µm x 8 µm images) of self-assembled PS-*b*-P2VP/NMP$^+$ I$^-$ with a targeted P2VP volume fraction of 55%.

Table S1. Normalized capacitance values for self-assembled PS*b*P2VP/NMP$^+$ I$^-$ BCEs on IDEs.

Targeted P2VP volume faction	**Time for CVIR (hours)**		
	6	**12**	**24**
45% P2VP	13.0 ± 0.3 pF nm^{-1}	12.7 ± 0.1 pF nm^{-1}	12.9 ± 0.3 pF nm^{-1}
47.5% P2VP	13.2 ± 0.3 pF nm^{-1}	13.0 ± 0.4 pF nm^{-1}	12.8 ± 0.1 pF nm^{-1}
50% P2VP	14.3 ± 0.4 pF nm^{-1}	15.0 ± 0.2 pF nm^{-1}	14.6 ± 0.2 pF nm^{-1}
52.5% P2VP	15.8 ± 0.2 pF nm^{-1}	16.1 ± 0.1 pF nm^{-1}	14.8 ± 0.5 pF nm^{-1}
55% P2VP	13.4 ± 0.9 pF nm^{-1}	13.2 ± 0.4 pF nm^{-1}	13.5 ± 0.4 pF nm^{-1}

Note: Average values for 3 samples. Standard error values reported.

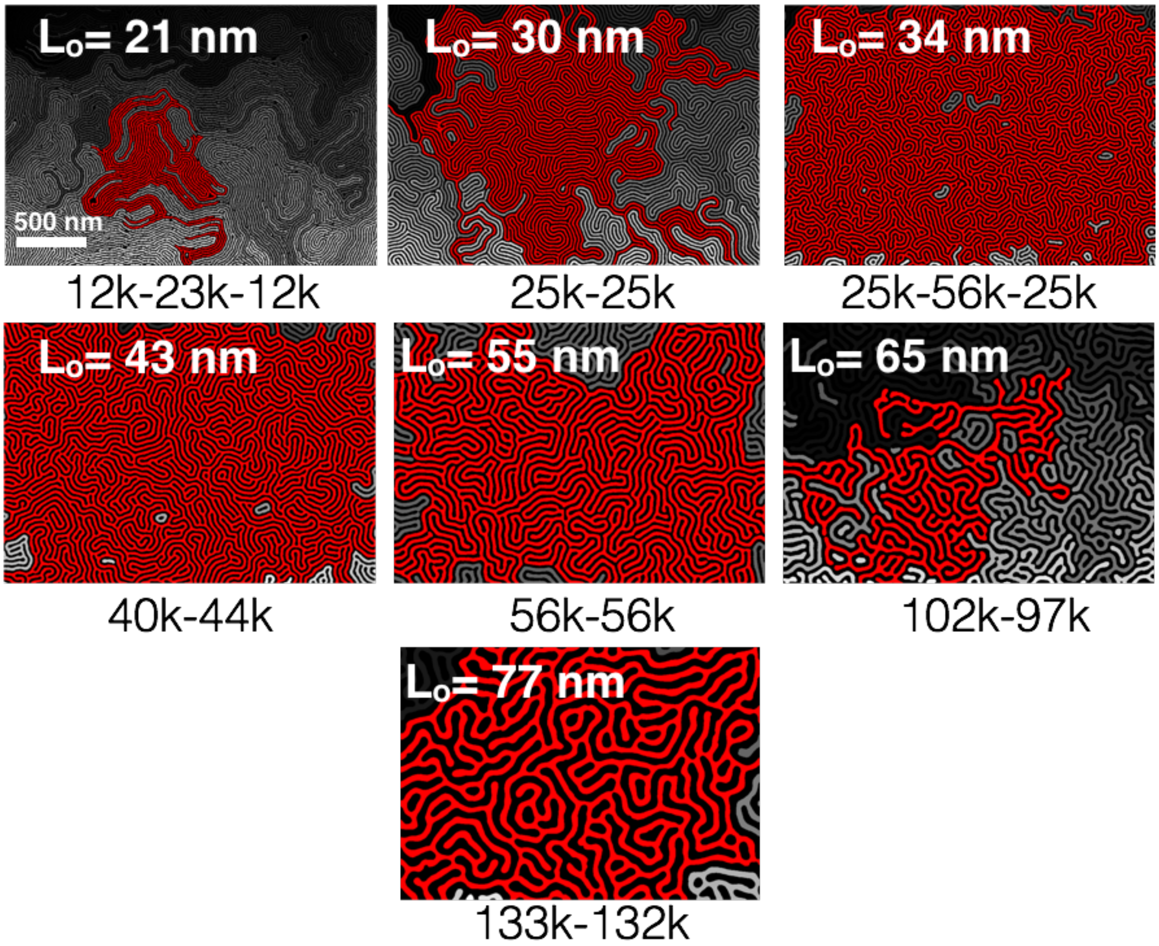

Figure S8. Processed SEM images of self-assembled BCEs with varying molecular weight. The red color indicates the largest connected P2VP/NMP$^+$ I$^-$ domain within the image. The molecular weight of the triblock or diblock copolymers in each of the images (in g/mol of each block) is shown under each image.

Table S2. In-plane conductivity, conversion of P2VP to P2VP/NMP$^+$ I$^-$, and IEC data for BCE thin film samples with varying M_n and morphological period.

M_n values	Period (nm)	Conversion	IEC (mmol g^{-1})	In-plane ionic conductivity σ (mS cm^{-1})	In-plane ionic conductivity normalized to IEC σ^*_N (mS cm^{-1}/mmol g^{-1})
12k-23k-12k	21	0.45 ± 0.00	1.66	15.2 ± 0.5	9.2
25k-25k	30	0.41 ± 0.00	1.52	14.2 ± 0.4	9.3
25k-56k-25k	34	0.43 ± 0.01	1.51	17.3 ± 0.5	11.5
40k-44k	43	0.42 ± 0.01	1.60	20.7 ± 0.6	12.9
57k-57k	55	0.41 ± 0.04	1.52	11.9 ± 0.3	7.8
102k-97k	65	0.41 ± 0.00	1.49	14.4 ± 0.6	9.7
133k-132k	77	0.41 ± 0.01	1.52	19.1 ± 0.1	12.6

Note: Average values for 3 samples. Standard error values reported.

To illustrate the importance of connectivity and to understand how the size of the morphological period *d* size influenced ionic conduction, we compared the ionic conductivity of diblock and triblock copolymer electrolytes with varying M_n values. Figure S8 depicts the processed SEM images for diblock PS-*b*-P2VP/NMP$^+$ I$^-$ and symmetrical triblock P2VP/NMP$^+$ I$^-$-*b*-PS-*b*-P2VP/NMP$^+$ I$^-$ samples of varying M_n values. The values of *d* for the different samples are provided in the SEM images and Table S2. All the different BCP variants were naturally PS rich without addition of homopolymer, and thus the degrees of ion domain connectivity in the samples were poor. Table S2 reports the P2VP to P2VP/NMP$^+$ I$^-$ conversion, IEC, in-plane iodide anion conductivity, and IEC normalized in-plane conductivity of the samples exposed to methyl iodide vapor for 24 h. No ionic conductivity trend with respect to *d* was observed. The lack of a trend between ionic conductivity and *d* for diblock and triblock PS-*b*-P2VP/NMP$^+$ I$^-$ samples was probably attributed to each sample displaying different degrees of ion domain connectivity, as seen in Figure S8. Our future work will look to investigate the influence of BCE period size and anion conductivity for P2VP rich systems.

Methods

Random copolymer synthesis

(PS-*r*-2VP)-OH random copolymers were synthesized by varying compositions of styrene (S) and 2-vinyl pyridine (2VP) via nitroxide-mediated controlled radical polymerization.[1] A representative polymerization procedure is described for the synthesis of copolymer as follows: a mixture of OH-modified initiator, S, and 2VP was degassed by three freeze-thaw cycles. The mixture was heated at 160 °C for 72 h under a nitrogen atmosphere. Conversion of both S and 2VP in the random copolymerization was determined to be greater than 95% in all cases. The resulting copolymers were dissolved in THF and then precipitated in hexanes. M_n was in the range of 2000-7500 g/mol, with PDI values of 1.2-1.6, and the fraction of S was determined by ^{1}H NMR spectroscopy.

Equations used to determine the amount of homopolymer to add to attain a targeted volume fraction

$$\bar{v}_i = \frac{(w_{i,BCP} f_i + w_{i,hp})\rho_{i,hp}^{-1}}{\sum_{i=1}^{2}(w_{i,BCP} f_i + w_{i,hp})\rho_{i,hp}^{-1}} \qquad \text{<S1>}$$

$$f_i = \frac{Mn_{i,block}}{\sum_{i=1}^{2}(Mn_{i,block})} \qquad \text{<S2>}$$

‘i’ = a particular block or homopolymer (hp) chemistry (e.g., PS or P2VP)

w_i = weight of BCP or hp added to the solvent mixture

ρ_i = density of the hp and the block material in the BCP ($\rho = 1.05$ g cm^{-3} for PS and $\rho = 1.114$ g cm^{-3} for P4VP) – values taken from Polymer Data Handbook[2]

$\bar{v}_i$ = targeted volume fraction in the BCP and hp mixture

f_i = mass fraction of a particular block in the BCP

Fabrication of substrates with SiN_x windows for STEM and RSoXS

Silicon wafers coated with SiN_x on both sides were patterned with a 10 x 10 array of rectangles on the SiN_x on the backside of the wafer. The patterned SiN_x would later serve as mask during KOH etching. Self-assembly of PS-*b*-P2VP diblock or triblock copolymers was then carried out on the front side of the wafer. Following the DSA process, the wafer was back etched using KOH wet etch procedure. With the front side of the wafer sealed and protected by a holder, the exposed silicon rectangles on the back side of the wafer was removed by KOH solution until the etching reached the silicon nitride on the front side, creating the imaging windows. The wafer was then cut up into individual windows for STEM imaging and RSoXS experiments.

Procedure to make IDEs

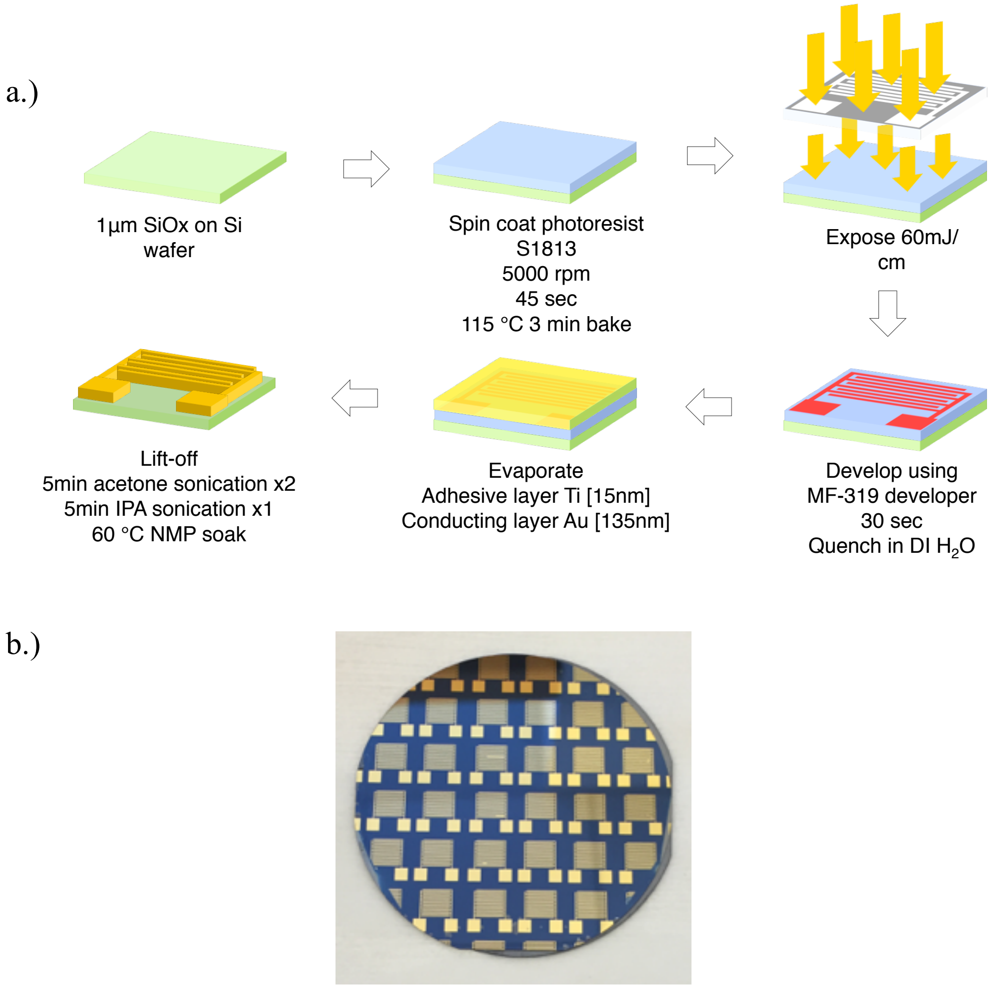

Figure S9. a.) Process flow diagram to make interdigitated electrodes (IDEs) using conventional photolithography. b) A picture of IDEs patterned on a two inch diameter silicon wafer with 100 µm thermally grown SiOx layer.

EIS measurements and ECE modeling

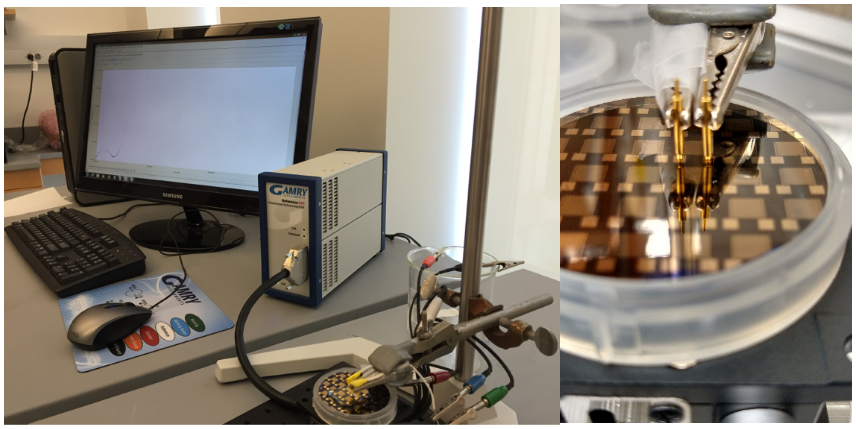

Figure S10. Photos of electrochemical testing of IDEs with Gamry Reference 600 Potentiostat/Galvanostat with Frequency Response Analyzer. A few drops of fresh deionized water (18.2 MΩ) is placed over the IDE being tested.

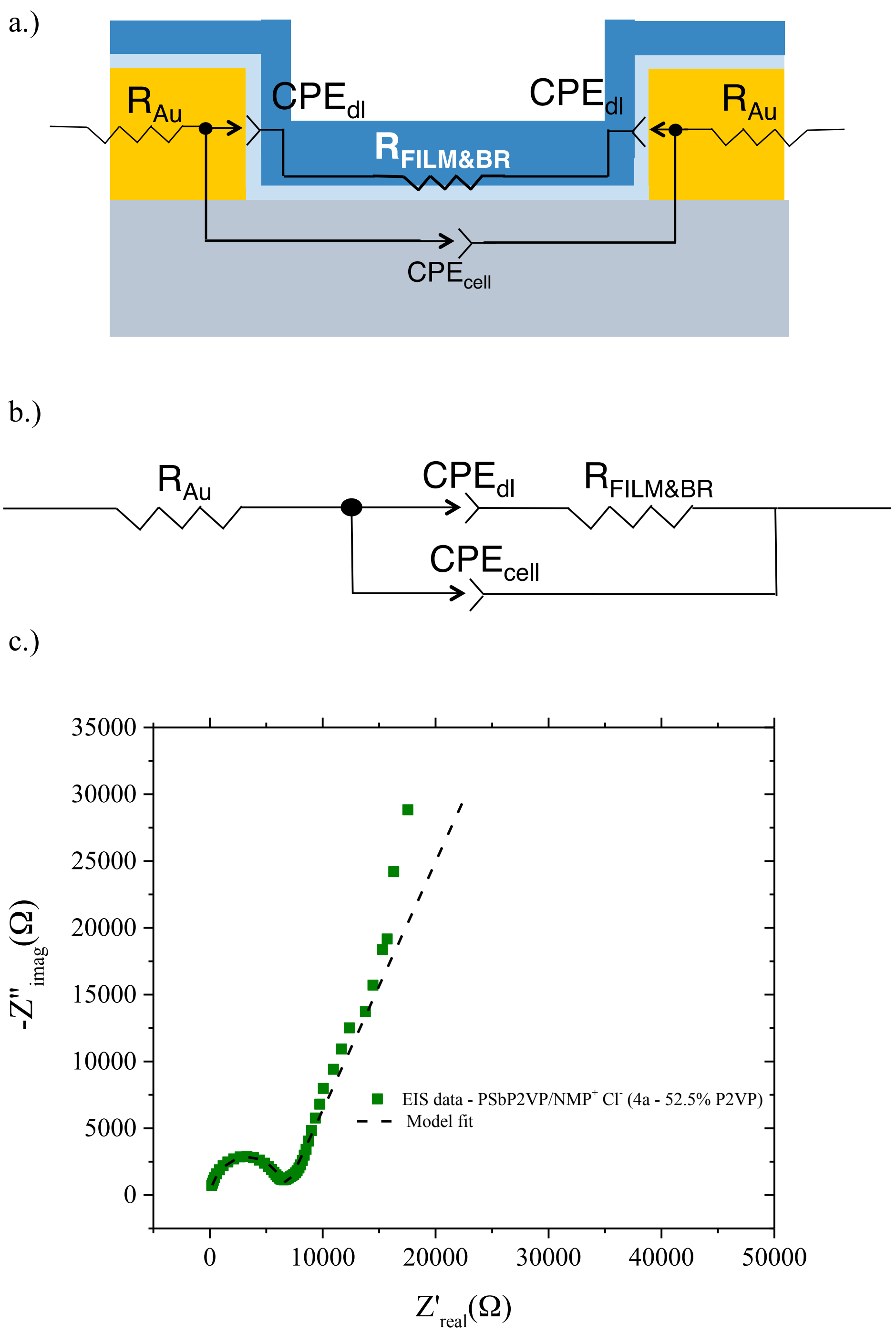

Figure S11. a.) Diagram of the integrated ECE model into IDE with BCE. b.) ECE model used to fit data in the Nyquist plot collected from EIS. c.) Model fit to EIS data in the Nyquist plot using Simplex Algorithm. The red underline in Panel C represents the BCE (i.e., film) and brush resistance and the calculated chloride ion conductivity of the sample is reported. Equation <S1> below was used to determine the chloride ion conductivity from the BCE (i.e., film) and brush resistance.

$$\sigma_{FILM\&BR} = \frac{1}{R_{FILM\&BR}} \cdot \frac{d}{l(n-1)t} \qquad \text{<S3>}$$

$R_{Film\&Br}$: the in-plane resistance of the BCE and brush layer
l: length of the teeth (0.45 cm)
t: thickness of the BCE film and brush layer (ranged from: nm to nm)
N: number of electrodes ($N = 22$)
d: interdigitated electrode teeth (100 μm)

$$C_{FILM\&BR} = \frac{1}{(Z_{CPE}(\omega=\omega_{max}))^{n} \cdot \omega_{max}} \cdot \frac{1}{t} \qquad \text{<S4>}$$

$C_{FILM\&BR}$: the BCE and brush layer capacitance
n: ideality of the capacitor (set equal to one for all model fits – assume ideal capacitor)
t: thickness of the BCE film and brush layer (ranged from: nm to nm)
ω: angular frequency
ω_{max}: angular frequency at the semicircle maximum

Equation <S3> was used to calculate the ionic conductivity of the thin film BCE film on an IDE, while equation <S4> was used to calculate the normalized capacitance of the thin film BCE.[3]

References

[1] P. Mansky, Y. Liu, E. Huang, T. P. Russell, C. Hawker, *Science* **1997**, *275*, 1458.
[2] J.E. Mark, *Polymer Data Handbook*, **1999**, Oxford University Press
[3] D. K. Paul, R. McCreery, K. Karan, *J. Electrochem. Soc.* **2014**, *161*, F1395.